

Henghui Zhang¹, Jichang Chen¹, Fangli Wang³, Guijia Zhang¹, Zishi Shen⁴, Qiang Zhu⁵, Guanghui Wu² & Mingbo Tong¹

¹Nanjing University of Aeronautics and Astronautics, Nanjing 210016, China ²Commercial Aircraft Corporation of China Ltd, Shanghai 201210, China ³Jinling Institute of Technology, Nanjing 211169, China ⁴Aircraft Strength Research Institute of China, Xian 710065, China ⁵China Special Vehicle Research Institute, Jingmen 448000, China

Abstract

Scale models play a crucial part in the tests to evaluate performance of amphibious aircraft. In the water landing process, it is necessary to consider the equal Froude number to satisfy the hydrodynamics similarity, and also the effect of Reynolds number on the aerodynamics. Therefore, evaluating the impact of scale effect on aircraft landing performance is a key issue in the water landing test of amphibious aircraft. In this paper, CFD simulation of aircraft models at different scales is carried out based on the Reynolds-Averaged Navier–Stokes equations (RANS) framework to explore and discuss the scale effects of aerodynamics and hydrodynamics. The simulation data was compared with the test data and showed good consistency. The computational results show that vertical acceleration and pitch angle changes have a linear decreasing trend as the scale decreases. And the water landing performance of the amphibious aircraft are discussed in detail based on the numerical analysis of water landing of the amphibious aircraft with different initial pitch angles. This study would give a better understanding of the deviation between the water landing tests and the real situation, and provide a reference basis for amphibious aircraft.

Keywords: scale effect, water landing, Reynolds effect, calm water

1. Introduction

Amphibious aircraft is a fixed-wing aircraft that can take off and land on water. Due to its unique ability of taking off and landing on water, amphibious aircraft can be competent for maritime patrol and rescue, maritime transportation, forest fire fighting and other work. At the same time, the safety of water landing has become one of the key issues considered by designers. In the process of water crash landing of amphibious aircraft, the bottom of the fuselage will be affected by a large water load, which tests the impact resistance of the aircraft, so it is particularly important to accurately evaluate the water characteristics.

At present, the research methods of aircraft landing mainly include theoretical calculation, experimental technique and numerical simulation. Due to the complex shape and the strong nonlinearity of the impact load, the theoretical calculation is generally difficult. Due to the size of the pool, it is difficult for the model used in the test to achieve the same size as the real aircraft, and the scale-down model is generally adopted, and the evaluation of the aircraft water landing performance in the real situation is limited by the scale effect, which will cause certain errors. Therefore how the results obtained using the scaled model can be used to forecast the real machine loads is a point of

interest. Due to the rapid development of computational fluid dynamics, numerical simulation methods play an increasingly important role in such problems. Since the bottom of a seaplane is similar to the hull of a ship, which is dominated by hydrodynamic drag, and the empirical formulas related to ships have been quite complete, the hydrodynamic formula of a ship is of great significance for calculating the hydrodynamic force of an amphibious. In 2017, Pereira et al [1] discussed the scaling effects of the KVLCC2 hull. Using 14 turbulence models available in the RANS solver, the scaling effects of nominal wake rate and shape factor were investigated. Instead of numerical validation in the experiments, the simulation errors of the numerical results with different turbulence models are compared. Finally, it is pointed out that the full-scale solution shows the robustness of the numerical method, while the model-scale solution has some modeling errors. In 2018, Boao Cai et al [2] considered that the scaling and real-vessel drag conversion method for conventional monohulls is not applicable to trimarans, and used numerical simulation to analyze four ship models with different scaling scales, and classified the drag force on trimarans into frictional drag, residual drag, and the sum of residual drag force on different bodies, to study the scale effect, resistance and the sum of resistance, to study the effect of scale effect on each resistance part of the three-hulled ship. In 2019, Sun et al [3] computationally investigated the viscous flow field of a ship at different scales by using the Reynolds number averaged Navier Stokes (RANS) method without considering the free-surface effect. The scaling effect of the nominal wake field is investigated. The wake fields of inner and outer propellers at different model scales were compared. In the same year, Kazerooni and Seif [4] proposed the scaling effect of high speed monohull hull drag. Modeling tests were conducted using two model scales. The drag components at different speeds and scales were given. And the experimental results were compared with other empirical methods. In 2019, Ke-wei Song [5] conducted a comprehensive study on the hydrodynamic performance of ships with and without tail flaps based on model tests and model and full-scale simulations. The model test and simulation results show that the installation of tail flaps can improve the wake flow field, thus reducing the ship's drag. Model-scale and full-scale simulation results show the different effects of tail flaps on the nominal wake of the ship. The results show that the full-scale numerical simulation method is more accurate in determining the performance of the tail flap compared to the model extrapolation method. Therefore, it is recommended that full-scale simulation should be used in the future design and research of medium- and high-speed ship tail appendages, such as tail flaps, tail wedges, interceptors, etc., to ensure that more accurate drag reduction ranges and rates are obtained. In 2019, Yao Huilan et al [6] retouched the scale effect conversion method proposed by the ITTC, and based on the numerical simulation method of the scaled-down model of a ship's propeller with different Reynolds numbers and the real propeller model analysis, proposed a correction method based on ITTC's conversion formula, and the repair method can get more accurate results relative to the original method. In 2020, Ali Dogrul et al [7] conducted URANS CFD simulations of KCS and KVLCC2 at different scales, investigated the effect of scale on the drag components, shape factor, wake field, and flow characteristics around the hull of the ship. The drag results obtained from the simulations were also compared with different drag extrapolation methods to check the compliance of different extrapolation methods for different hulls. In 2024, Cheng JC et al [8] by fixing the Froude number, five geosim cases with different scale factors are carried out based on the Reynolds-Averaged Navier-Stokes equations (RANS) framework. Results also show that the scale effect is mainly introduced by the dissimilarity of Reynolds number, which leads to the discrepancies of boundary layer, wave surface elevation and flow separation between the scale model and prototype.

In this paper, the numerical simulation method based the Reynolds-Averaged Navier–Stokes equations (RANS) framework is used to calculate the landing process of amphibious aircraft in static water under different scales. The effects of different scale reduction on the water landing performance characteristics are mainly discussed, and effects of different pitch angles on response characteristics of amphibious aircraft water landing are analyzed.

2. Computational Method

2.1 Governing Equations and Numerical Schemes

The numerical analyses are conducted using STAR-CCM+, which solves unsteady Reynolds-Averaged Navier-Stokes (RANS) equations. The governing equations can be given as:

$$\frac{\partial \rho}{\partial t} + \frac{\partial (\rho u_i)}{\partial x_i} = 0 \tag{1}$$

$$\frac{\partial(\rho u_i)}{\partial t} + \frac{\partial}{\partial x_i}(\rho u_i u_j) = -\frac{\partial p}{\partial x_j} + \frac{\partial}{\partial x_j} \mu(\frac{\partial u_i}{\partial x_j} - \rho \overline{u_i' u_j'}) + S_j$$
 (2)

where u_i and u_j denote the time-averaged values (i, j = 1, 2, 3) of the velocity component; P is the time-averaged value of the pressure; P is the fluid density; P is the dynamic viscosity coefficient; P is the Reynolds stress term; and S_i is the source term.

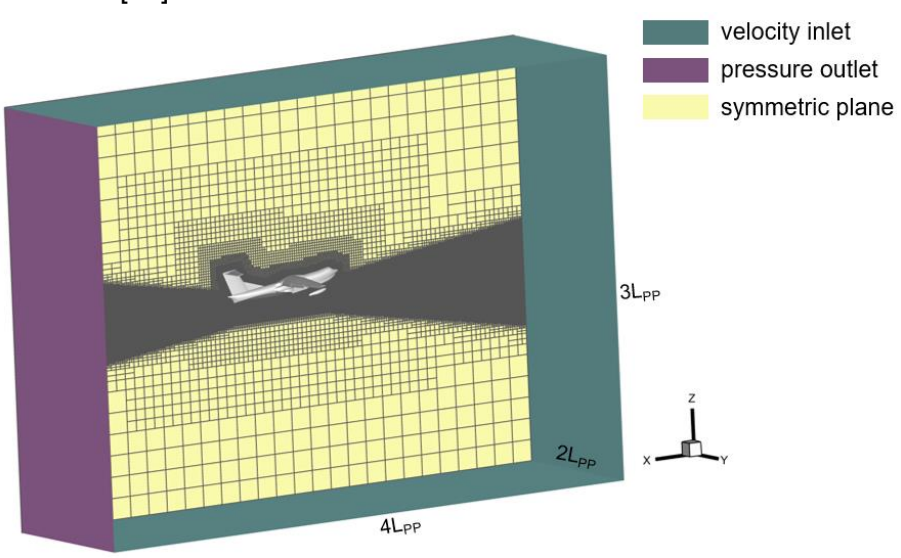
The shear-stress transport (SST) k-w turbulence model was used to simulate the strong adverse pressure gradient flow field [9]. The formulation based on pressure; second-order upwind spatial discretization and second-order central discretization were used for the convective flux terms and diffusion terms.

In order to capture the change of free liquid surface efficiently and improve the calculation accuracy of body force, VOF method is used to determine the free surface of air—water interface [10].

2.2 Computational Domain and Boundary Conditions

Considering the computational cost, the symmetry of the model allows us to use half-mode calculation, and the size and dimensions of the computational domain are (length \times width \times height) $4L_{PP}\times2L_{PP}\times3L_{PP}$. Referring to the studies conducted by Song et al (2021) [11]. The boundary conditions are set to simulate the flow field under real conditions. The inlet, top, bottom and side are the velocity inlet, the outlet is the pressure outlet, and the middle of the fuselage is the symmetric plane, as shown in the Figure 1[12].

The flow field mesh moves with the body to achieve an accurate prediction of the amphibious aircraft motion. A reasonable custom function of volume fraction is applied to the boundary. Due to the large pitch angle movement of the aircraft in water landing process, the area near the aircraft body and the sector areas swept by the front and rear fuselage are encrypted. The grid heights are $0.002\ L_{PP}$, $0.002\ L_{PP}$ and $0.005\ L_{PP}$ [13].



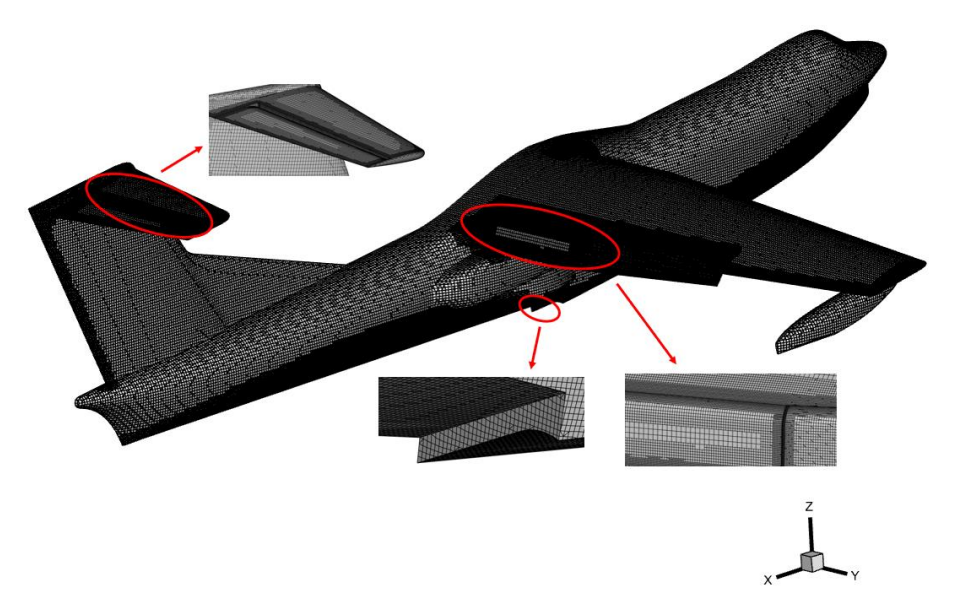


Figure 1 – Boundary conditions and mesh generation strategies

2.3 Calculation Model Parameters

The aircraft will be affected by both aerodynamics and hydrodynamics in the process of water landing. Hydrodynamic resistance mainly includes viscous resistance and wave making resistance. The coefficient of viscous resistance is mainly related to the Reynolds number. And the wave resistance coefficient is mainly due to the wave generation of the surrounding water surface driven by the movement of the aircraft, so that the surrounding water pressure change causes additional water resistance, which is mainly related to the Froude number. The Reynolds number (Re) and Froude number (Fr) are expressed as follows[14]:

$$R_e = \frac{ul_{wing}}{v} \tag{3}$$

$$F_r = \frac{u}{\sqrt{gl_{hull}}} \tag{4}$$

where u is the velocity of the aircraft, l_{wing} and l_{hull} are respectively the aerodynamic and hydrodynamic reference length, v is the kinematic viscosity of the air, g is the gravity.

Table 1: Simulation matrix of different scale factors at Fr 1.53.

Parameters	λ			
	1	1/4	1/8.5	1/16
u_x , Horizontal velocity (km/h)	105.16	52.58	36.07	26.29
u_z , Descent velocity (km/h)	17.52	8.76	6.01	4.38
$l_{\it wing}$, Aircraft MAC(m)	38.76	9.69	4.56	2.175
$l_{\it hull}$, Aircraft hull length (m)	36.98	9.24	4.35	2.31
Re, Reynolds number	9.01×10^{6}	1.13×10^{6}	3.63×10 ⁵	1.41×10^{5}

Since the scaling laws of Reynolds number and Froude number cannot be satisfied at the same time. There will be errors between the scale model and the actual model obtained in the water landing test. In this study, the influence of scale effect on water landing performance is analyzed under the premise

that the Froude number is the same. The conversion relationship of water landing velocity corresponding to different scale factors is as Table 1.

3. Results and discussion

3.1 Comparisons Between Numerical Results and Test Data in Model Scale

When $\lambda=8.5$, the process of water landing of amphibious aircraft is calculated based on the method in Section 2. The initial pitch angle of the aircraft is 6°, the horizontal velocity is 36.07 Km/s, and the descent velocity is 6.01 Km/s. The numerical simulation results were compared with the test results in literature. As shown in Figure 2, the change curve of the vertical acceleration and the aircraft pitch angle time history of the fuselage within 0.7s of aircraft landing time is shown.

The coincidence between the numerical simulation results and the experimental results of vertical acceleration time curve is high. The peak value of time history curve of pitch angle increases relatively by 1° and the peak time comes out earlier. The reason is that the free fall motion of the whole aircraft model studied in this paper is different from the model in water landing test. The motion process is affected by the wing aerodynamic force.

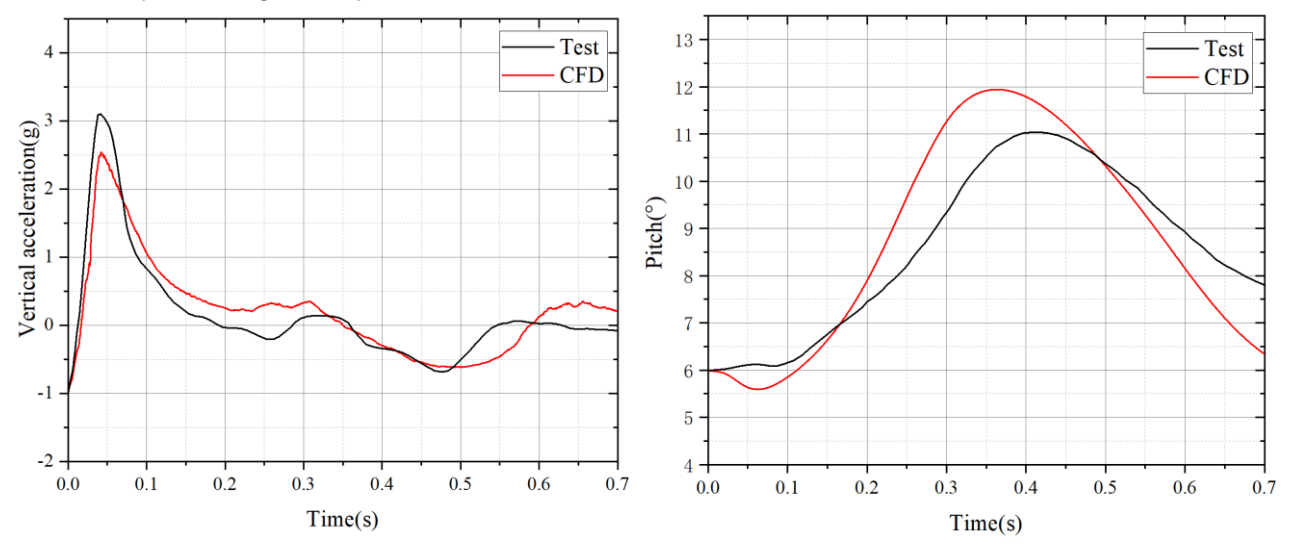


Figure 2 – Comparison of time-history results between numerical results and test data

3.2 Scale Effect on Water Landing Performance

The water landing performance of the amphibious aircraft when the scale λ =1, 4, 8.5, 16 is calculated. As shown in Figure 3, the vertical acceleration of aircraft water landing is remarkably influenced by the scale factor. It shows consistent variation rules with different scaling scales. The two peaks of the vertical acceleration in the real model change linearly as the scale decreases. The first peak can be simulated accurately by the scale model, the peak value is reached at T =0.044s. The vertical acceleration is decreased from 2.504g to 2.482g as the model reduces in size from λ =1/1 to λ =1/16, difference of 0.9%.The error of the second peak is larger, and the value of the vertical acceleration decreases from 0.72g to 0.135g. As shown in Figure 4, the change curve of the aircraft pitch angle time history of the fuselage is shown. The variation trend of the pitch angle of different models is the same. But the peak value of the pitch angle obtained by the scaled models is smaller than that of the real plane model. As the model reduces, the peak value gradually decreases from 12.524°to 11.733°, the error is 6%.

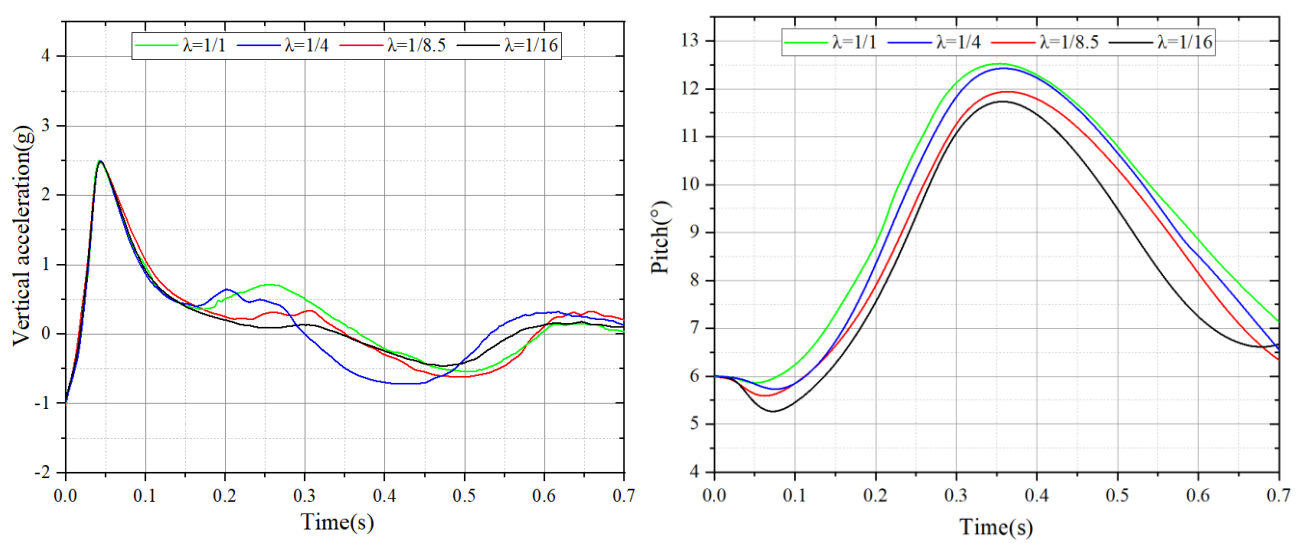


Figure 3 – Results of amphibious aircraft water landing when the scale λ =1, 4, 8.5, 16

3.3 Effect of Initial Pitch Angle on Water Landing Characteristics

The water landing process of amphibious aircraft with initial pitch angle of 4° , 6° and 8° is simulated with the scale model when λ =8.5. To explore the variation rule of acceleration and pitch angle, the numerical simulation physics time length is 0.7s[15]. Fig.4 shows the change process of vertical acceleration and pitch angle time history. The change trend of vertical acceleration is basically the same. When initial pitch angle is 4° , the peak overload is 2.64g, which is obviously larger than the other cases. As the initial pitch angle decreases, the vertical acceleration peak value decreases linearly, and the change of pitch angle during the aircraft landing becomes larger. and the maximum change of pitch angle occurs when the initial pitch angle is 4° , with a change value of 6.67°. The initial pitch angle of 6° has a maximum pitch angle of 11.94° at t = 0.363s.

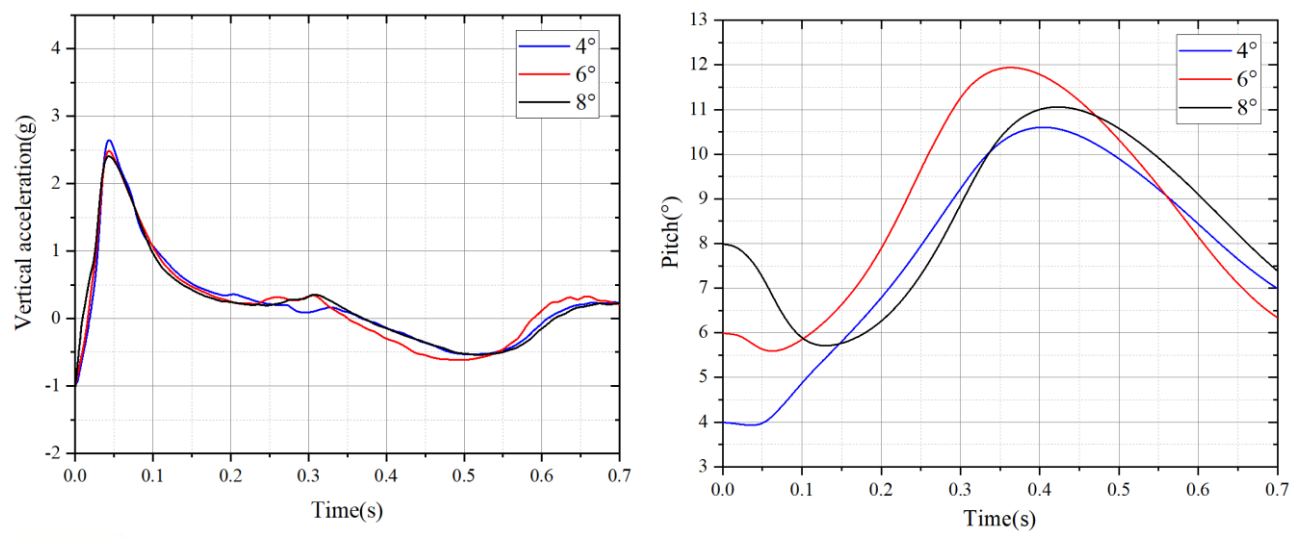


Figure 4 – Results of amphibious aircraft water landing with initial pitch angle of 4°, 6° and 8°

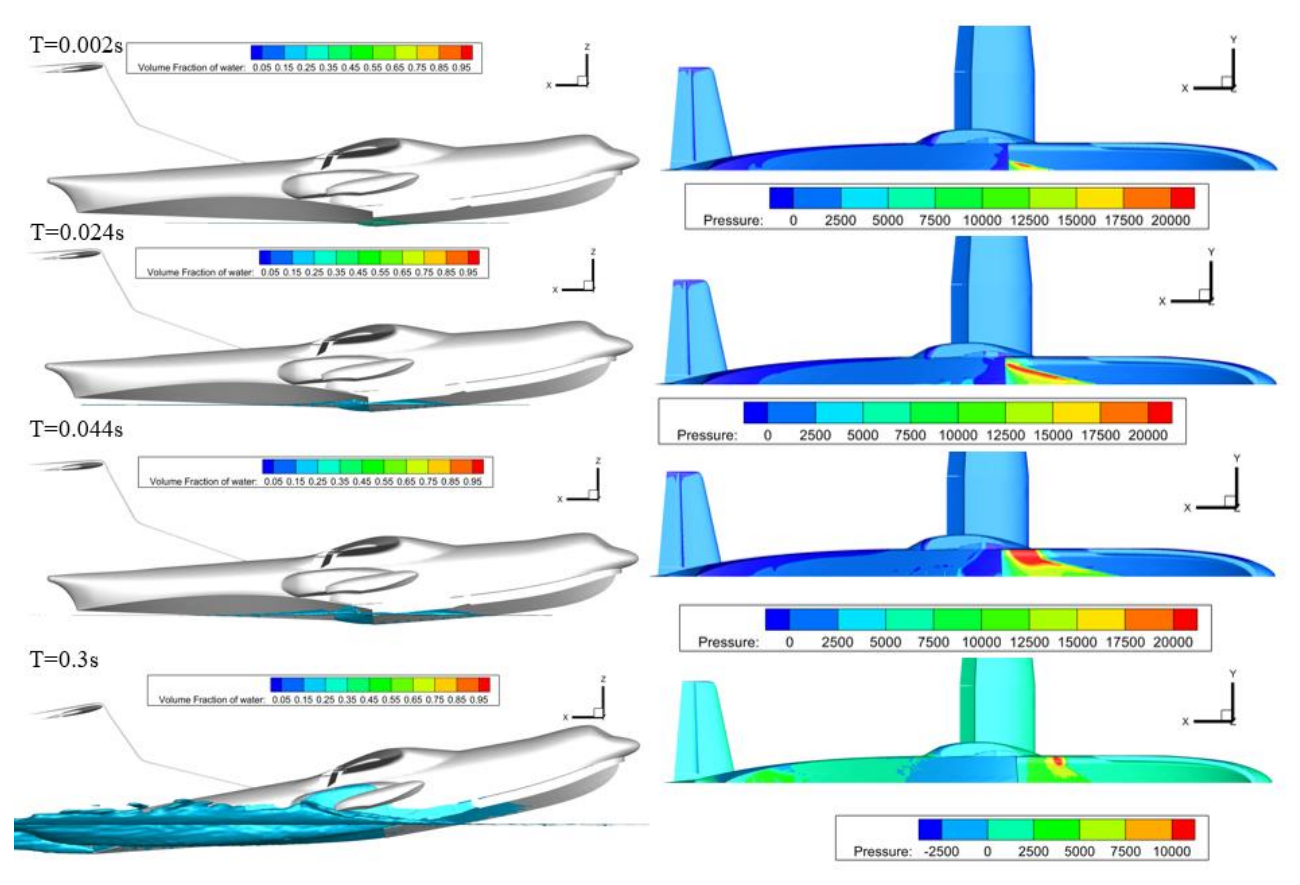


Figure 5 – Landing motions and pressure contours of bottom when initial pitch angle=4°

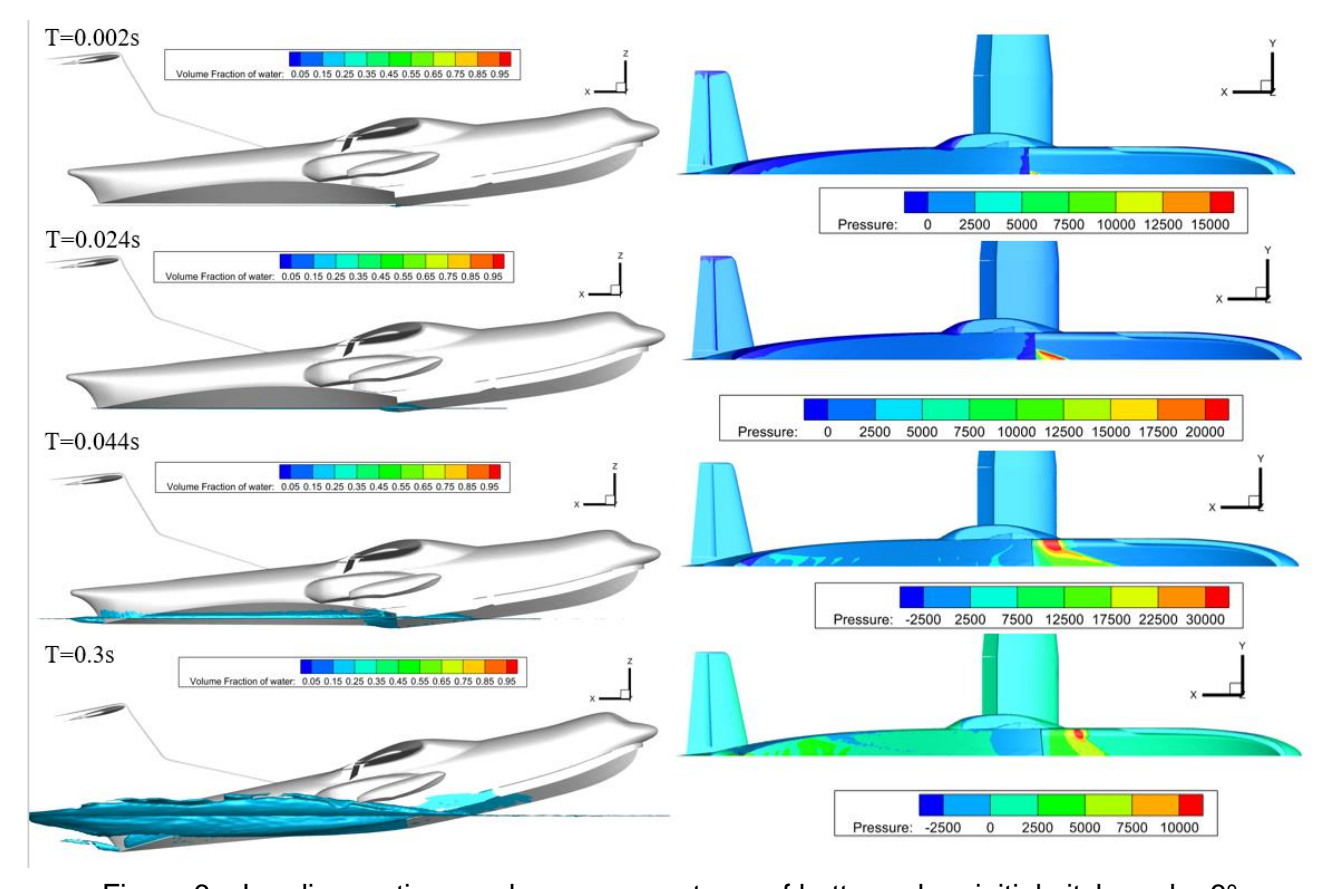


Figure 6 – Landing motions and pressure contours of bottom when initial pitch angle=6°

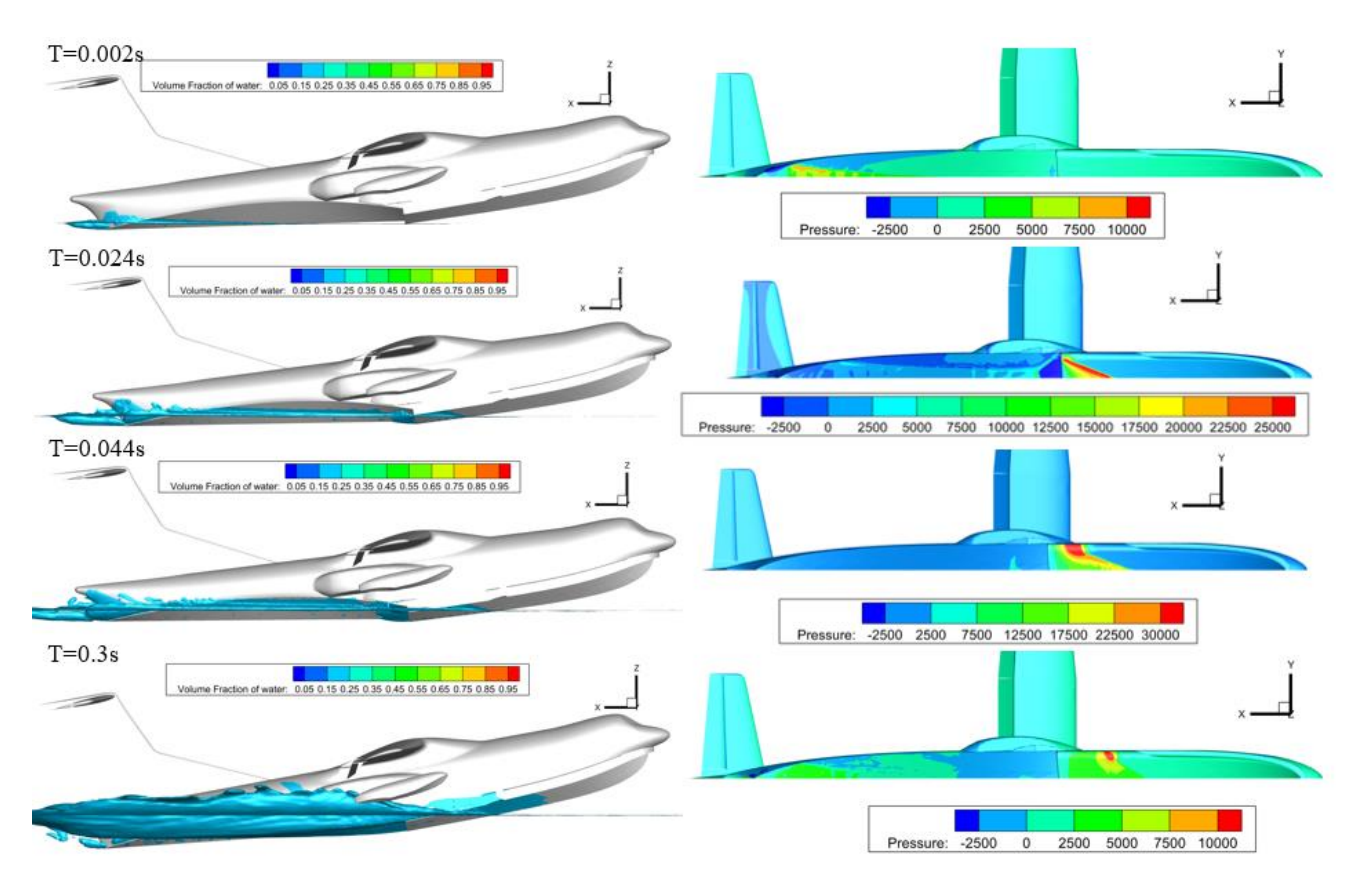


Figure 7 – Landing motions and pressure contours of bottom when initial pitch angle=8°

It is worth mentioning that when the initial pitch angle was 8°, the airplane appeared a large forward pitch before t = 0.13, and the pitch angle decreased by 2.29°. Figures 5-7 show the water surface position cloud and pressure cloud of the amphibious airplane at T= 0.002s, 0.024s, 0.044s, 0.3s. And we find that the tail part of the airplane fuselage firstly touches the water at T =0.02s, which leads to a forward pitching moment, leading to the occurrence of this phenomenon. Combining the cloud diagrams, we can derive another universal rule that when an amphibious airplane lands on water, the vertical overload of the fuselage increases at the same time with the increasing area of water touching, and reaches the maximum overload when the area of water touching is the largest. Before the overload is reached, the high-pressure area appears on the gliding surface of the forward body of the step and gradually moves to the bow. And the negative pressure area always exists in the stern and a small part of the area after the step during the whole process. This phenomenon is not obvious due to the fact that the stern touches the water first at the initial pitch angle of 8°. When the secondary peak is reached, the rear section of the fuselage touches water basically, but the secondary peak is smaller because of the reduced planing speed.

4. Conclusion

Numerical simulation of the hydrostatic landing process of an amphibious aircraft is carried out numerically by the RANS method from the design and experimental point of view. The effects of scale effect and different initial pitch angles on the water landing performance of amphibious aircraft are investigated. Based on the results obtained, the following conclusions can be drawn.

- 1. The numerical simulation model developed in this paper is in good agreement with the experiments, Based on this method, the analysis of amphibious aircraft water landing process can provide an effective means for amphibious aircraft load forecasting.
- 2. The scale effect has little impact on the overall trend of the wave landing performance, includes

amplitude levels of vertical acceleration and pitch angle. In particular, the maximum peak load, which is the most important concern during flooding, was predicted with an error of only 0.9%. This feature can provide useful guidance for the use of small-scale models in the early stages of amphibious aircraft design.

3.During the water landing of amphibious aircraft, the vertical acceleration of the fuselage increases with the increase of the water touching area, and the vertical acceleration of the fuselage reaches the maximum when the water touching area is maximum. Negative pressure areas appear at the tail of the fuselage and behind the step during water landing.

5. Acknowledgments

The research content of this article has been supported by Aeronautical Science Foundation of China, project number:20230023052001,20220023052001.

6. Contact Author Email Address

Prof. Dr. Mingbo Tong

College of Aerospace Engineering

Nanjing University of Aeronautics and Astronautics

#29 Yudao Street, Qinhuai District, Nanjing City, Jiangsu Province

Zip code:210016

Email: tongw@nuaa.edu.cn

7. Copyright Statement

The authors confirm that they, and/or their company or organization, hold copyright on all of the original material included in this paper. The authors also confirm that they have obtained permission, from the copyright holder of any third party material included in this paper, to publish it as part of their paper. The authors confirm that they give permission, or have obtained permission from the copyright holder of this paper, for the publication and distribution of this paper as part of the ICAS proceedings or as individual off-prints from the proceedings.

References

- [1] Pereira F; Vaz G; Eca L. Verification and Validation Exercises for the Flow Around the KVLCC2 Tanker at Model and Full-Scale Reynolds Number. Ocean Engineering, Vol.129, pp 133–148, 2017.
- [2] Cai BA; Qin JT; Mao X. Influence of Scale Effect on Resistance Components of Trimaran. Journal of Wuhan University of Technology, Vol.42, pp 487-491. 2018.
- [3] Sun S; Chang X; Guo C; et al. Numerical investigation of scale effect of nominal wake of four-screw ship[J]. Ocean Engineering, Vol.183, pp 208-223, 2019.
- [4] Fathi Kazerooni; Seif M S. On the scale effects of resistance model tests of high-speed monohulls[J]. Journal of the Brazilian Society of Mechanical Sciences and Engineering, Vol.41, 2019.
- [5] Song K; Guo C; Wang C; et al. Numerical analysis of the effects of stern flaps on ship resistance and propulsion performance. Ocean Engineering, Vol.193, 2019.
- [6] Qin HL, Zhang HX. Improvements of Scaling Method Recommended by ITTC at a Lower Reynolds Number Range. Journal of Shanghai Jiaotong Universit, Vol.5, pp 35-41, 2019.
- [7] Dogrul A.; Song S.; Demirel Y K. Scale effect on ship resistance components and form factor. Ocean Engineering, Vol.20 ,2020.
- [8] Chen JC, Le L, Fu XQ, Xiao TH, Wu B, Tong MB. Scale effect on wave planing performance of amphibious aircraft at constant speed. Aerospace Science and Technology, Vol.148 ,2024.
- [9] Elhanafi, A.; Fleming, A.; Leong, Z.; Macfarlane, G. Effect of RANS-based turbulence models on nonlinear wave generation in a two-phase numerical wave tank. Prog. Comput. Fluid Dyn 17, pp 141–158,2017.
- [10]Hirt, C.W.; Nichols, B.D. Volume of fluid (VOF) method for the dynamics of free boundaries. *Comput.Phys*,39, pp 201–225,1981.
- [11] Song K W, Guo C Y, Wang C, et al. Experimental and numerical study on the scale effect of stern flap

- on ship resistance and flow field. Ships and Offshore Structures, 2019.
- [12]Song KW, Guo CY, Gong J, Li P, Wang LZ. Influence of interceptors, stern flaps, and their combinations on the hydrodynamic performance of a deep-vee ship. Ocean Eng,170, pp 306–320,2018.
- [13] Chen JC, Xiao TH, Wu B, Wang FL, Tong MB. Numerical study of wave effect on water entry of a three-dimensional symmetric wedge. Ocean Engineering, Vol. 250, pp 0029-8018,2022.
- [14]Sun F, Wu B, Lian ZD, Wang MZ, Chu LT. Influence of pitch angle on water-entry performance of large-scale amphibian aircraft hull. Journal of Ship Mechanics, Vol. 23, pp 397-404, 2019.
- [15]Lu YJ, Xiao TH, Deng SH, Zhi HL, Zhu ZH, Lu ZY. Effects of initial conditions on water landing performance of amphibious aircraft. Chinese Journal of Aeronautics, Vol. 42, pp 159-170, 2021.